RESEARCH REPORTS
Biomaterials & Bioengineering

J.E. Schmitz[1#], J.D. Teepe[2#], Y. Hu[3], C.E. Smith[3,4], R.J. Fajardo[1], and Y.-H.P. Chun[5*]

[1]Department of Orthopaedics, RAYO, Carlisle Center for Bone and Mineral Imaging, School of Medicine, University of Texas Health Science Center at San Antonio, USA; [2]Dunn Dental Clinic, Lackland Air Force Base, San Antonio, TX, USA; [3]Department of Biologic and Materials Sciences, University of Michigan, Dental Research Lab, Ann Arbor, MI, USA; [4]Department of Anatomy & Cell Biology, McGill University, Montreal, PQ, Canada; and [5]Department of Periodontics, Dental School, University of Texas Health Science Center at San Antonio, 7703 Floyd Curl Drive, San Antonio, TX 78229, USA; [#]authors contributing equally to this publication; *corresponding author, chuny@uthscsa.edu

Estimating Mineral Changes in Enamel Formation by Ashing/BSE and MicroCT

J Dent Res DOI: 10.1177/0022034513520548

APPENDIX

Mineral Density Calibration

Three hydroxyapatite (HA) phantoms (0.25, 0.75, and 2.927 g/cm^3) were used to calibrate enamel mineral density measurements from the linear attenuation coefficient (LAC) values. The 2 lower density phantoms were provided by Bruker Skyscan (Aartselaar, Belgium) and were composed of HA and resin. The highest density phantom was created through a sintering process, and its density was reported as 2.9 g/cm^3 (Himed, Old Bethpage, NY, USA). The density of this phantom was independently confirmed by ashing to remove residual moisture and other non-mineral materials in the disc. The disc mass did not change after ashing at 600° C (Pyradia, F100, Longueuil, QC, Canada).

The intra- and inter-specimen variances of the 2.9 g/cm^3 phantoms were determined by μCT with 4 volumes of interest (VOIs) *per* phantom (Appendix Table 2). Phantoms were scanned at the same settings as the hemi-mandibles to determine their volume and LAC. The average LAC was 0.145891. The average volume for the phantoms by μCT was 0.03192439 cm^3. The intra- and inter-specimen LAC variances were small, indicating that the 2.9 g/cm^3 calibration phantoms were homogenous within and between samples. The dry weight of the phantoms was determined by the ashing technique as previously described, and the average mass was found to be 0.09345 g. The average mineral density of the phantoms was therefore 2.92723 g/cm^3. The standard curve of the average mineral densities and LAC values for all 3 phantoms indicated a strong linear relationship ($R^2 = 0.997$) (Appendix Fig. 4).

Radial Peel and Minimizing Partial Volume Boundary Effects

To assess the boundary and partial volume effects, we measured the LAC using different pixel peel values (0-3). A peel is a radial erosion of the volume of interest by a pre-determined number of pixels. A radial 2D pixel peel was used to reduce the effects of partial volume averaging at the enamel organ boundaries. Four peel settings were used and the differences between them determined by paired *t* tests (Appendix Fig. 5). The average enamel densities for each peel across all segments were the following: peel 0 = 2.3441 (± 0.8078), peel 1 = 2.3692 (± 0.8214), peel 2 = 2.3719 (± 0.8221), and peel 3 = 2.3716 (± 0.8196). Significant differences were found for several comparisons in most segments, indicating that VOI size influenced enamel density results, albeit by less than 1.2% in all instances. A one-pixel peel was used in all analyses. This pixel peel was chosen because it amounted to a 10-μm total erosion in any transect of the enamel (all surfaces lost a pixel = 5 μm). Since the average thickness of the enamel in ES3 and ES4 was approximately 100 μm, the peel represented a removal of 10% of the enamel. We avoided using a larger peel because this would remove a greater percentage of this absolutely small enamel structure. Although 2 and 3 pixel peels increased the mineral density, the differences with a single pixel peel were only 0.11%, at best. As expected, the lowest average enamel density was observed when no peel was applied.

Statistical Analysis of Enamel Mineral Density

We calculated the mean enamel mineral density from mineral weight and volume for corresponding ESs using either data from ashing, BSE, or μCT. Mineral density for μCT was determined *via* LAC. Statistical comparisons were performed by analysis of variance (ANOVA) with Tukey-Kramer *post hoc* comparisons. When variances were unequal, Wilcoxon ranks and pairwise comparison tests were used. From ESs 1 through 6, no statistical differences within corresponding ESs were found (Appendix Table 3). Overall, the enamel mineral densities corresponded well for the different methods. Statistical discrepancies ($p < .05$) were found for ES 7 and 8 between μCT/BSE and μCT/μCT. Mineral densities in mature enamel reached 2.81 and 2.97 mg/mm^3 when estimated from mineral weight by μCT and volume by BSE or μCT.

Appendix Table 1. Inter- and Intra-operator Variance

	Absolute Differences and Percentage Differences			
	Inter-operator		Intra-operator (COV)	
	Enamel Mineral Density	Volume	Enamel Mineral Density	Volume
Early Maturation				
Actual	0.01235 (± 0.00932)	0.00221 (± 0.00113)*		
%	1.7 (± 1.5)	6.6 (± 3.6)	0.9	4.1
Mid-maturation				
Actual	0.01469 (± 0.01911)	0.00184 (± 0.00218)		
%	1.0 (± 1.5)	5.5 (± 6.2)	0.1	1.5
Late Maturation				
Actual	0.00639 (± 0.00374)	0.00107 (± 0.00088)		
%	0.2 (± 0.1)	3.5 (± 2.9)	0.1	0.9

Two skilled operators manually contoured one ES in the early, mid-, and late maturation stages for 5 WT mandibles. For one operator, these volumes of interest were repeated 4 times to assess precision. Inter-operator discrepancies reported as mean (± SD). Intra-operator variability reported as coefficient of variation (COV). Actual = the mean of the absolute difference. % = the mean of the percentage difference between operators. * $p \leq .05$.

Results reported as mean (± SD). Intra-operator variability reported as Coefficient of Variation (COV). Actual = The mean of the absolute difference. % = The mean of the % difference between operators. * Indicates significant difference between operators ($p < .05$).

Appendix Table 2. Intra- and Inter-specimen Variance of the High-density Phantoms

	Linear Attenuation Coefficients (cm^{-1})					
	VOI 1	VOI 2	VOI 3	VOI 4	Intra-specimen Variance	Mean
Phantom 2	0.13973	0.14308	0.14426	0.14495	0.000005	0.143005
Phantom 3	0.14662	0.14671	0.14662	0.14665	0.000000	0.146650
Phantom 4	0.15018	0.15022	0.15038	0.15001	0.000000	0.150197
Phantom 5	0.14653	0.14553	0.14349	0.13931	0.000010	0.143715
Inter-specimen Variance	0.00002	0.00001	0.00001	0.00002	0.000004	0.145891

Four high-density phantoms were obtained from Himed (Old Bethpage, NY, USA). After each phantom was scanned 4 volumes of interest (VOIs) were generated, and the linear attenuation coefficient (LAC) was determined.

Appendix Table 3. Enamel Mineral Density (mg HA/mm^3)

	Ash/BSE (mg/mm^3)		Ash/μCT (mg/mm^3)		μCT/BSE (mg/mm^3)		μCT/μCT (mg/mm^3)	
Enamel Segment Number	Mean	SD	Mean	SD	Mean	SD	Mean	SD
1	0.19	0.12	–		–		–	
2	0.36	0.12	–		–		–	
3	0.60	0.18	0.68	0.21	0.63	0.16	0.70	0.08
4	1.11	0.32	1.19	0.35	1.17	0.32	1.26	0.33
5	1.85	0.29	2.05	0.32	1.84	0.23	2.07	0.36
6	–		–		2.39	0.13	2.66	0.20
7	–		–		2.62*	0.16	2.91*	0.07
8	–		–		2.81*	0.23	2.97*	0.05

Mineral densities of enamel were calculated from mineral weight divided by volume for each ES. Mineral weight was derived from ash weight (Ash) or μCT. Volumetric data were derived from BSE or μCT. * $p \leq .05$.

Appendix Table 4. Time Requirement by Modality

Time Requirement by Modality	Microdissection	μCT
Step 1: Specimen Preparation, Data Acquisition	Strip dissection/incisor: 2 days	Scan/hemimandible: 2 hr Reconstruction: 10 min
Step 2: Processing	Ashing: 1.7 days	Contouring VOI: 45 min
Step 3: Data Analysis	4-6 hr	4-6 hr
Total time for 1 specimen	94-96 hr	7-9 hr

A comparison between the times required for microdissection and μCT. μCT offers large time savings over microdissection in the measurement of mineral content and mineral density.

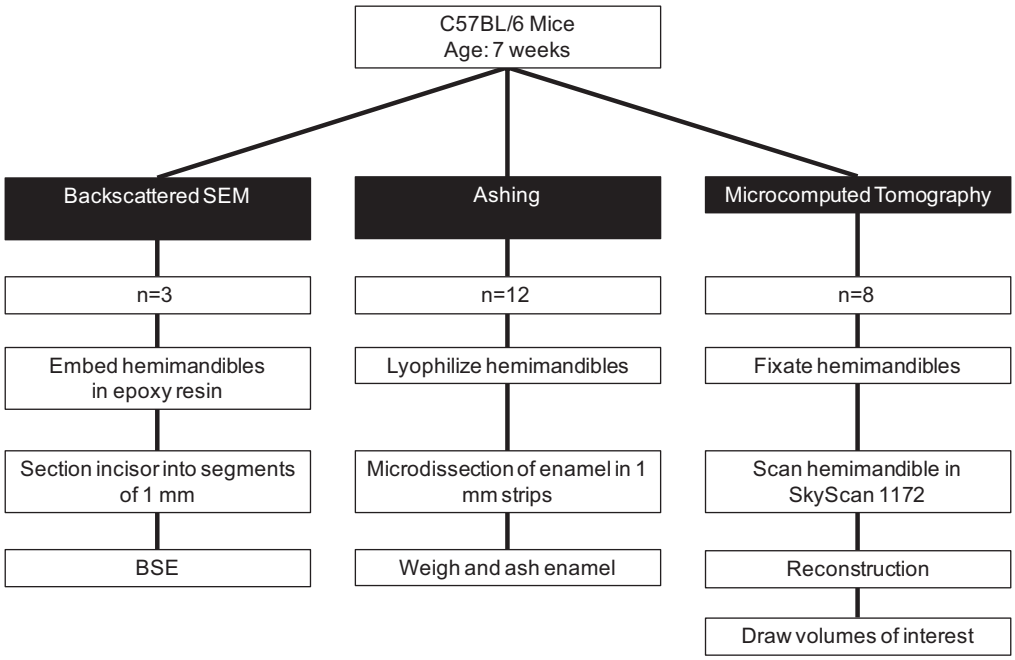

Appendix Figure 1. Overview of the work flow of the study. Different C75BL/6 mice were used for backscattered SEM (n = 3), ashing (n = 12), and μCT (n = 8).

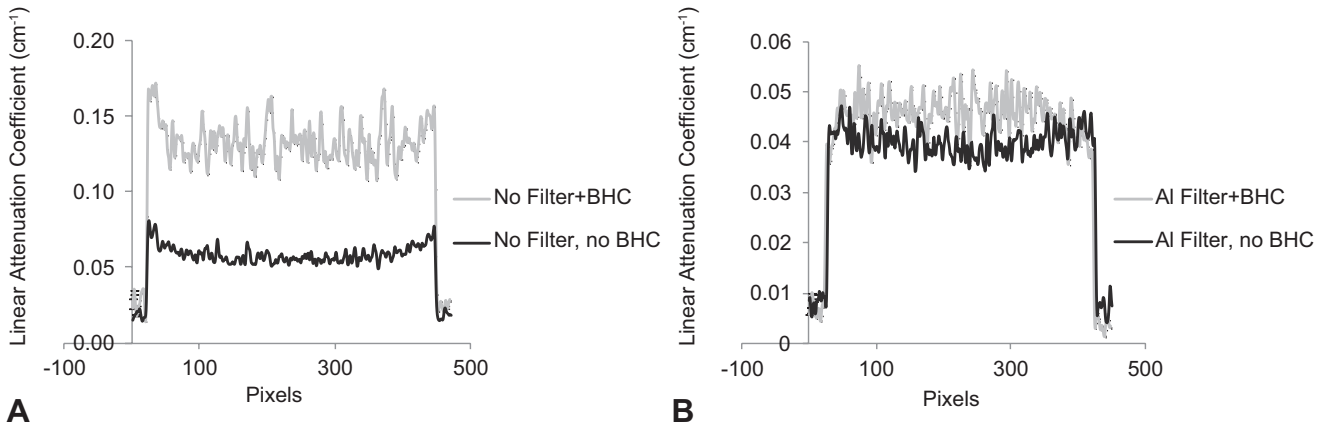

Appendix Figure 2. Effects of filter and beam-hardening correction on linear attenuation coefficient (LAC) of the medium density phantom. The 0.75 g/cm^3 phantom was scanned **(A)** without and **(B)** with an aluminum filter. All other settings except exposure time were held constant (Meganck *et al.*, 2009). The 2 scans were reconstructed twice, first without implementation of a beam-hardening correction (BHC) (dark gray) and a second time with the BHC (light gray). Profile lines were drawn through the center of each scan, and the LAC was plotted. Beam-hardening (cupping artifact) is clearly present in the image data acquired without filtration (A) and in the image data reconstructed without the BHC (dark gray in B). The cupping artifact was greatly mitigated by aluminum filtration of the polychromatic beam and reconstruction with a polynomial BHC (Kovács *et al.*, 2009).

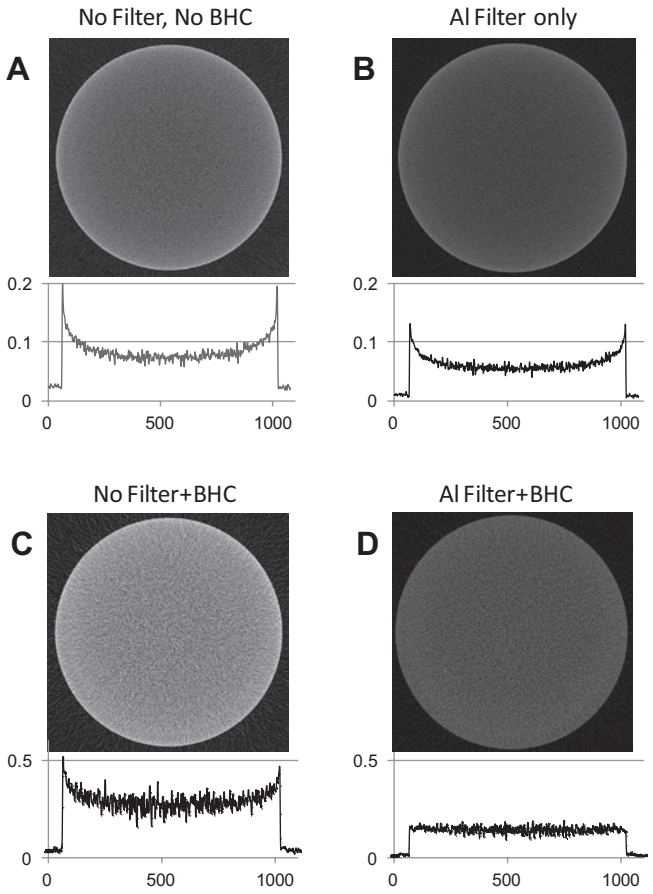

Appendix Figure 3. Effects of filter and beam-hardening correction on linear attenuation coefficient (LAC) of the high-density phantom. The high-density phantom was scanned without (**A** and **C**) and with an aluminum filter (**B** and **D**). All other settings except exposure time were held constant (Meganck *et al.*, 2009). The 2 scans were reconstructed twice, first without implementation of a beam-hardening correction (BHC) (A and B) and a second time with the BHC (C and D). Profile lines were drawn through the center of each scan, and the LAC was plotted. Beam-hardening (cupping artifact) is clearly present in the image data acquired without filtration (A and C) and in the filtered image data reconstructed without the BHC (B). The cupping artifact (D) was greatly mitigated by aluminum filtration of the polychromatic beam and reconstruction with a polynomial BHC (Kovács *et al.*, 2009).

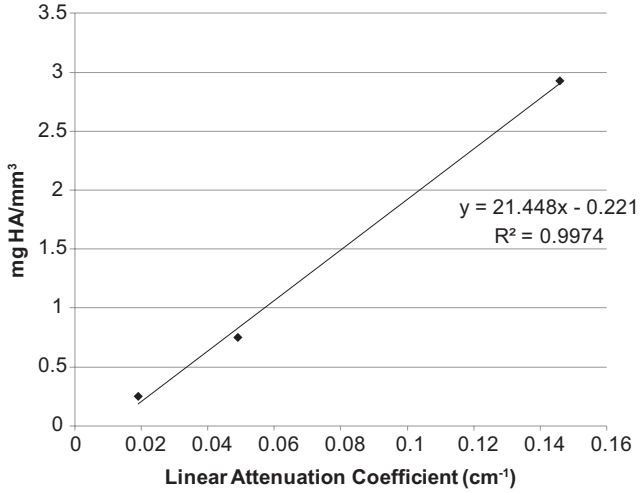

Appendix Figure 4. Determination of enamel mineral density from the linear attenuation coefficient (LAC) values of phantoms.

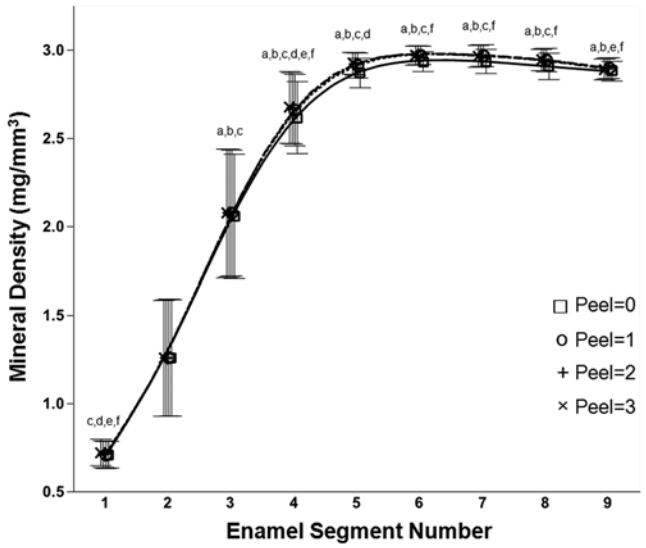

Appendix Figure 5. Effect of peel applied to volume of interest on linear attenuation coefficient (LAC). [a]$p < .05$ for Segments 0 and 1, [b]$p < .05$ for Segments 0 and 2, [c]$p < .05$ for Segments 0 and 3, [d]$p < .05$ for Segments 1 and 2, [e]$p < .05$ for Segments 1 and 3, and [f]$p < .05$ for Segments 2 and 3.

Inter- and Intra-operator Variability

Enamel mineral density inter-operator differences were low and non-significant for all comparisons. Enamel volume inter-operator differences were non-significant in the mid- and late maturation stages, but the discrepancy was significant in the early maturation stage ($p = .011$). Differences in both variables decreased with increasing mineralization (Appendix Table 1).

APPENDIX REFERENCES

Kovács M, Danyi R, Erdélyi M, Fejérdy P, Dobó-Nagy C (2009). Distortional effect of beam-hardening artefacts on microCT: a simulation study based on an in vitro caries model. *Oral Surg Oral Med Oral Pathol Oral Radiol Endod* 108:591-599.

Meganck JA, Kozloff KM, Thornton MM, Broski SM, Goldstein SA (2009). Beam hardening artifacts in micro-computed tomography scanning can be reduced by x-ray beam filtration and the resulting images can be used to accurately measure BMD. *Bone* 45:1104-1116.